PREPARED IN COOPERATION WITH THE
BUREAU OF RECLAMATION AND THE NATIONAL PARK SERVICE

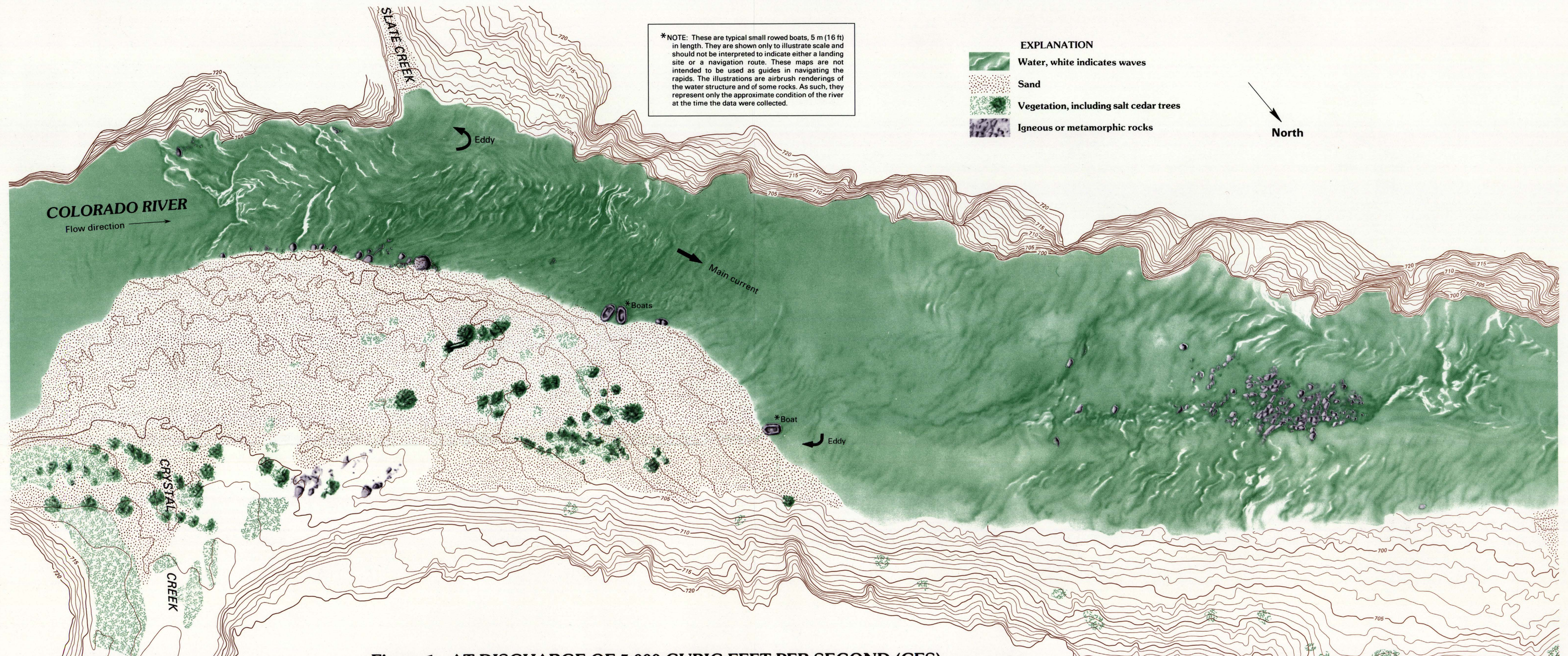

Figure 1—AT DISCHARGE OF 5,000 CUBIC FEET PER SECOND (CFS)

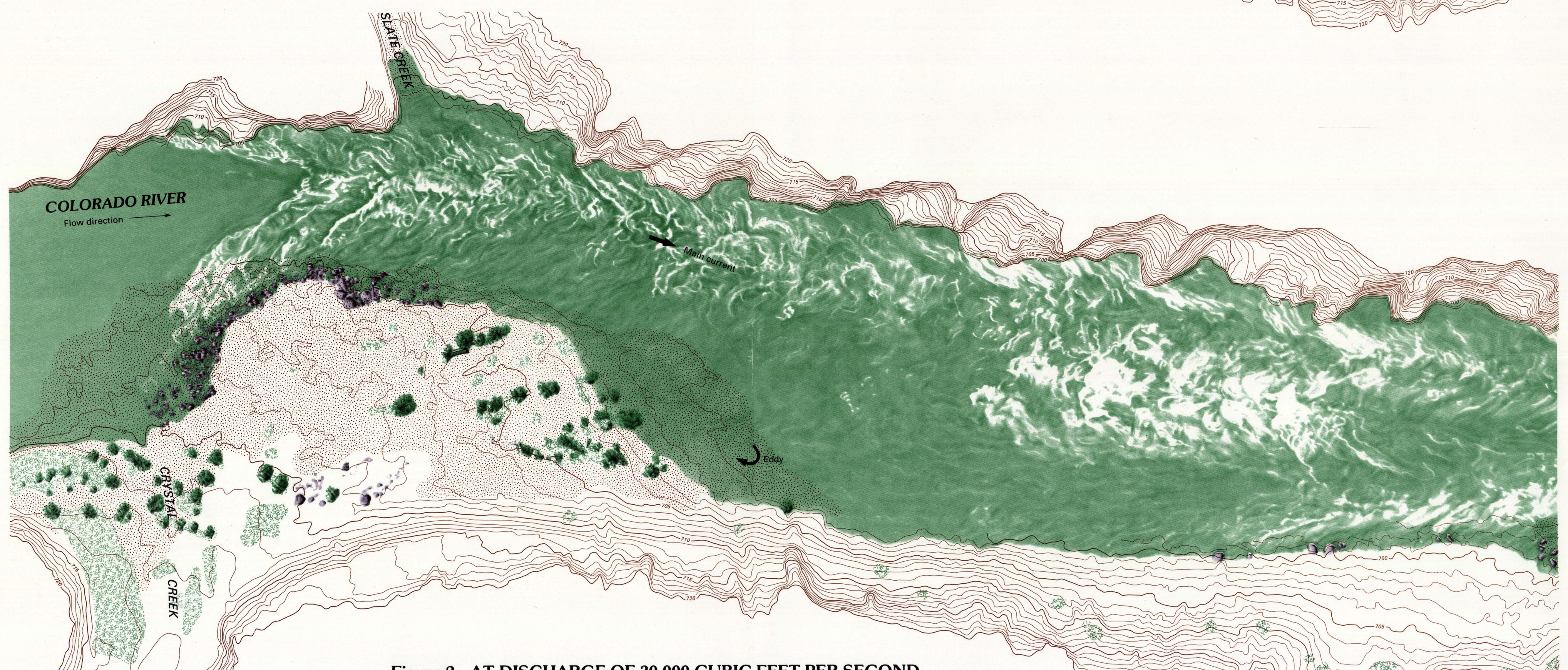

Figure 2—AT DISCHARGE OF 30,000 CUBIC FEET PER SECOND

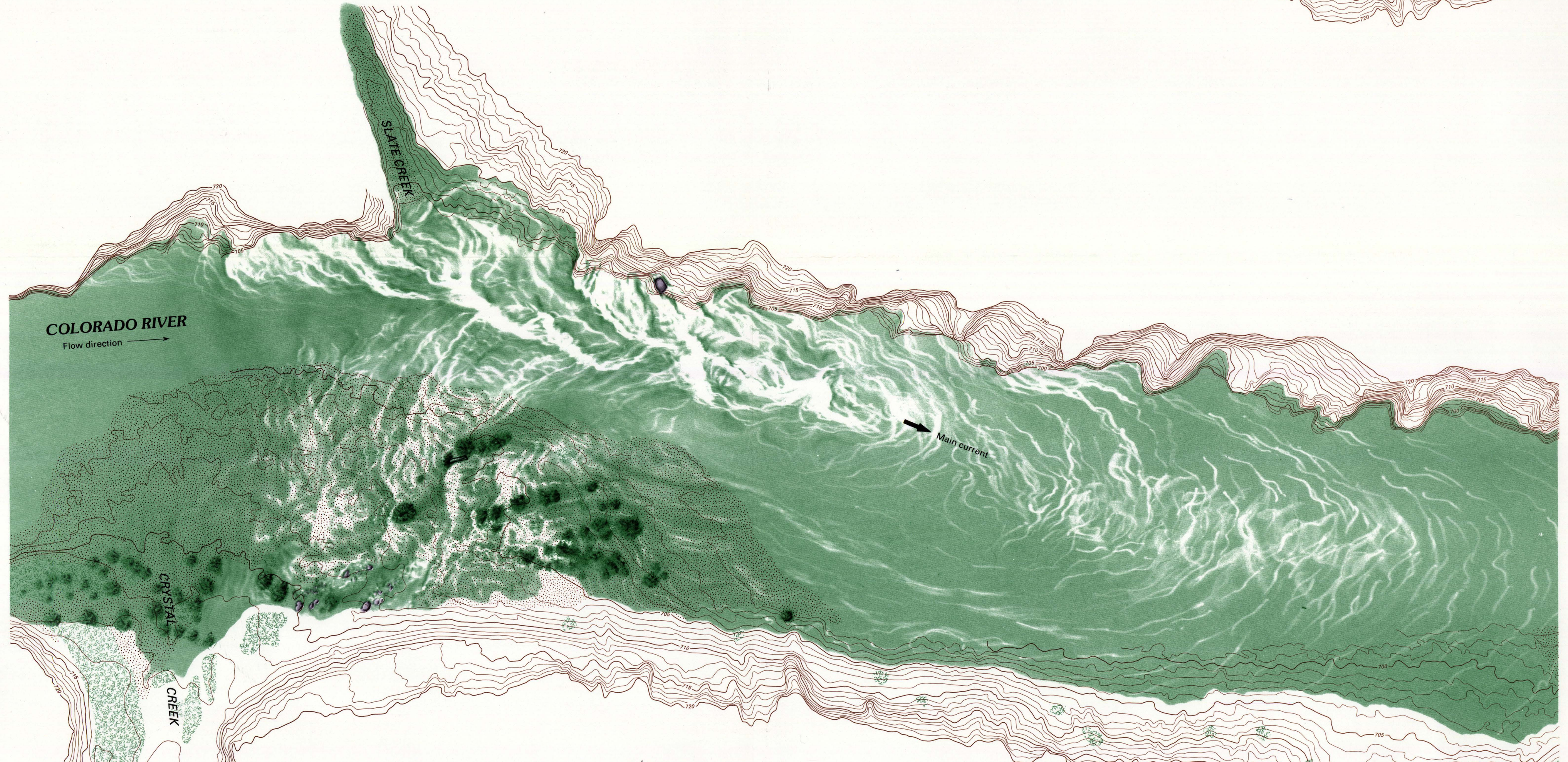

Figure 3—AT DISCHARGE OF 92,000 CUBIC FEET PER SECOND

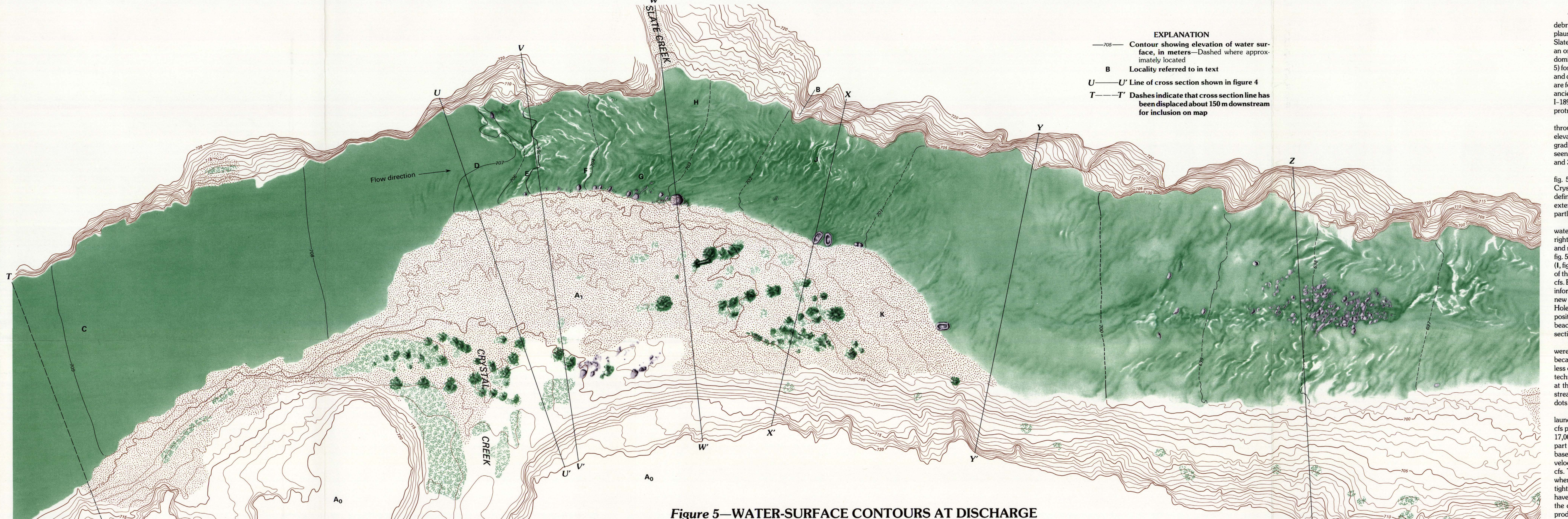

Figure 5—WATER-SURFACE CONTOURS AT DISCHARGE OF 5,000 CUBIC FEET PER SECOND

Figure 6—FLOAT VELOCITIES AT 7,000 CUBIC FEET PER SECOND ON BASE OF 5,000 CUBIC FEET PER SECOND

EXPLANATION

4.6 4.5 Average velocity between points, in meters per second—Bar over number indicates average for multiple streamlines.

(4.2–5.1) Indicates range of measured velocities

700 Contour showing elevation of water surface, in meters—Dashed where approximately located

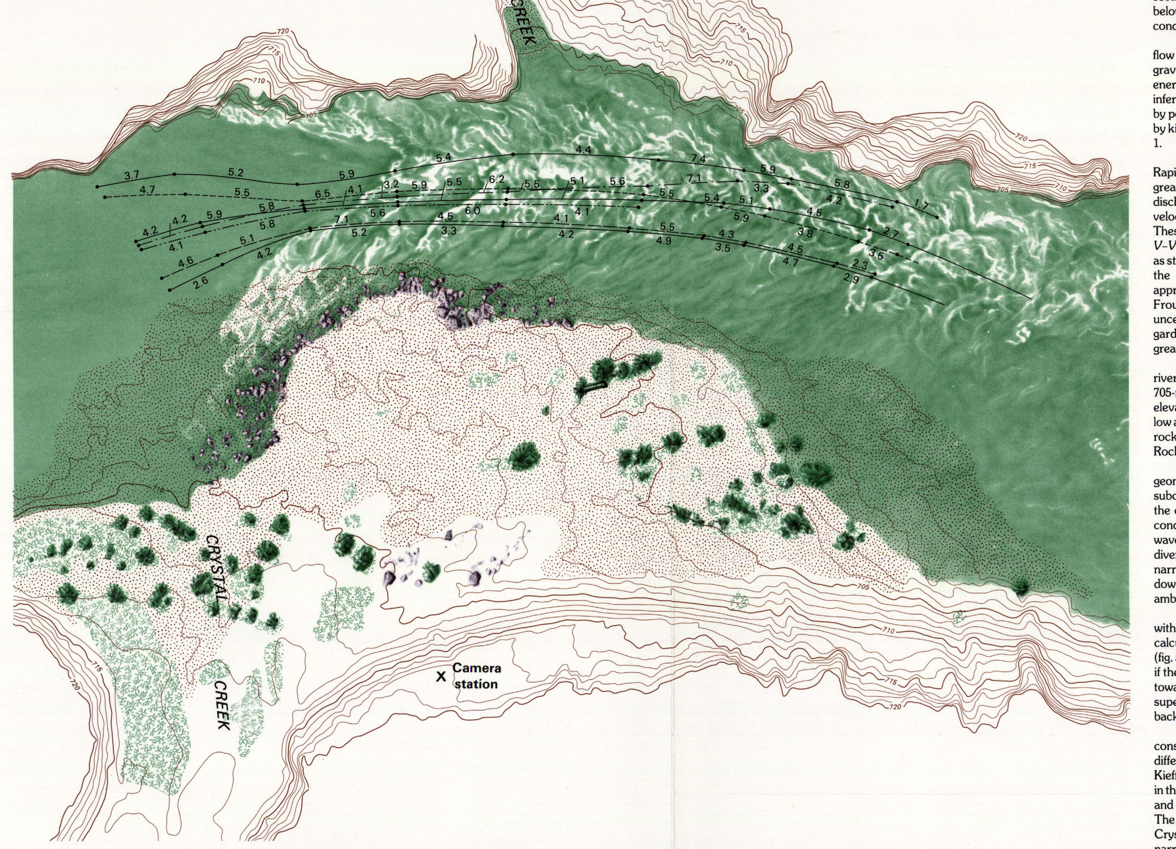

Figure 7—FLOAT VELOCITIES AT 17,000 CUBIC FEET PER SECOND ON BASE OF 30,000 CUBIC FEET PER SECOND

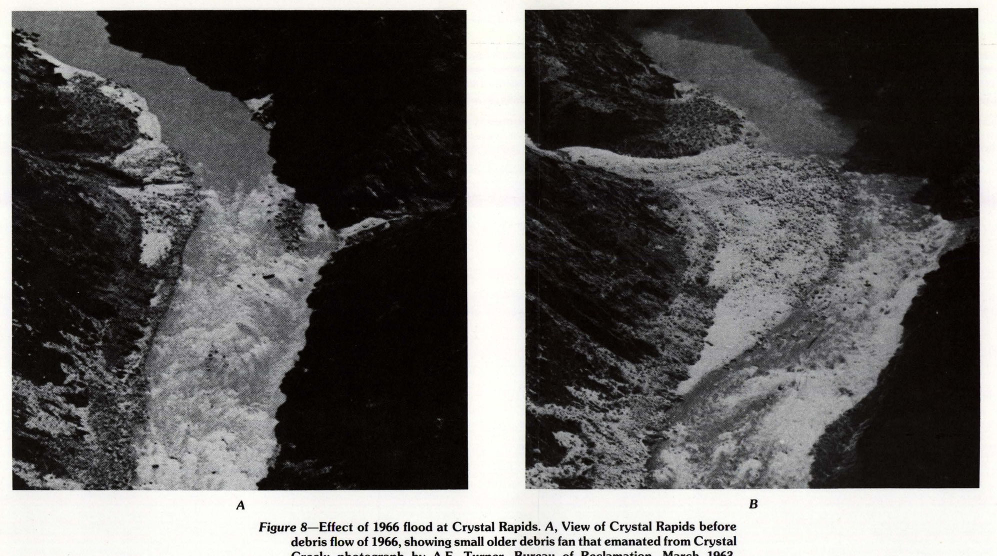

Figure 8—Effect of 1966 flood at Crystal Rapids. *A*, View of Crystal Rapids before debris flow of 1966, showing small older debris fan that emanated from Crystal Creek; photograph by A.E. Turner, Bureau of Reclamation, March 1963. Discharge estimated at 5,000 to 6,000 cfs. Corresponds to setting illustrated schematically in figure 9*E*. *B*, Same view after the December 1966 debris increased the size of debris fan. Photo taken March 1967 by Mel Davis, Bureau of Reclamation. Discharge is 16,000 cfs. Corresponds schematically to setting illustrated in figure 9*C* or *D*.

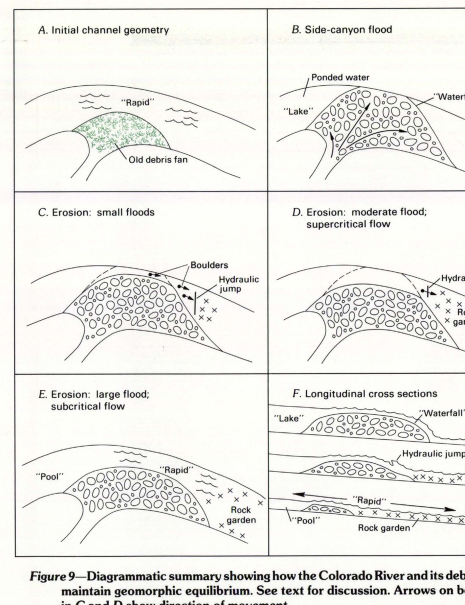

Figure 9—Diagrammatic summary showing how the Colorado River and its debris fans maintain geomorphic equilibrium. See text for discussion. Arrows on boulders in *C* and *D* show direction of movement.

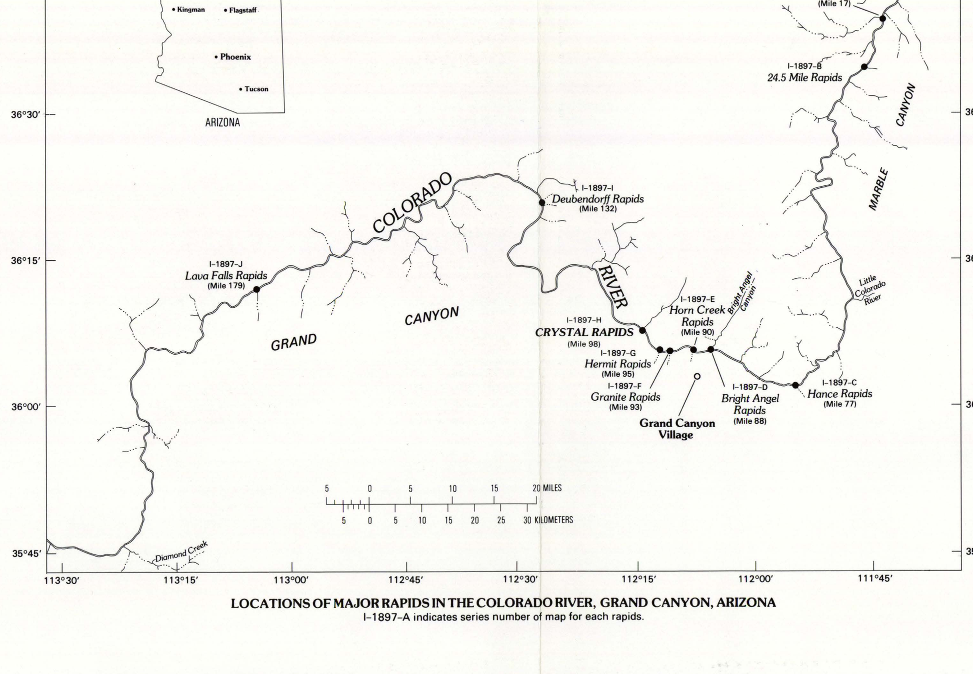

LOCATIONS OF MAJOR RAPIDS IN THE COLORADO RIVER, GRAND CANYON, ARIZONA
I–1897–A indicates series number of map for each rapids.

INTRODUCTION

The current configuration of Crystal Rapids (figs. 1, 2, 3 and 4) is caused by a series of debris flows from Crystal Creek on the north side of the Colorado River, although it seems plausible that in the past the rapid could have been strongly influenced by debris flows from Slate Creek on the south side of the river. The drainage area of Crystal Creek is approximately an order of magnitude larger than that of Slate Creek, so flows from Crystal Creek probably dominate the configuration of Crystal Rapids most of the time. The current debris fan (**A₁**, fig. 5) forces the Colorado River against the south wall of the canyon, a wall of predominantly mica and quartzo-feldspathic schist of the Vishnu Group. Remnants of an older dissected alluvial fan are found as terraces about 15 m above the river (**A₀**, shown in two locations on fig. 5). Similar ancient, dissected fans occur at Lava Falls (see Map I–1897–J) and at Hance Rapids (Map I–1897–C.) The nearly vertical foliation of the schist produces many resistant buttresses that protrude into the river (for example, at **B**, fig. 5).

At a discharge of 5,000 cubic feet per second (cfs), the elevation of the water surface through the rapid drops 11 m through the area mapped in this study (from about 708-m to 697-m elevation; fig. 5). Of this 11 m, a drop of 4 m occurs at the top of the rapid. The slope (average gradient) of the water surface through the rapid decreases as the discharge increases, as can be seen by a comparison of the water-surface elevations above and below the rapid in figures 1, 2, and 3.

Upon approach toward Crystal Rapids, the main channel flow turns into a backwater (**C**, fig. 5); this backwater is affectionately dubbed "Lake Crystal" by river runners. Although Crystal Rapids and this backwater have existed for a very long time, the backwater was definitely enlarged when debris flow **A₁** (fig. 5) was emplaced in 1966. The backwater now extends upstream to Boucher Rapids, a distance of nearly 1 mile, and Boucher Rapids was partly drowned by the enlargement of the backwater in 1966.

The acceleration of water into Crystal Rapids begins in the constriction. A smooth path of water, referred to as the "tongue" (**D**, fig. 5), is bounded on both sides by oblique waves. On the right side of the tongue is a set of three waves (**E**, **F**, and **G**, fig. 5), which have different heights and strengths at different discharges. A strong eddy circulates at the mouth of Slate Creek (**H**, fig. 5). The shear zone between this eddy and the main current can produce a tall curling wave (**I**, fig. 5) at high discharges (see figs. 2 and 3). Downstream near the end of the constricted part of the rapid, a trough and wave form a major boating hazard at discharges above about 10,000 cfs. Before 1983 this feature was known as the "Crystal Hole", and since 1983 it has been known informally as the "Old Crystal Hole" (**J**, fig. 5); the change in informal name arises because the new waves **E**, **F**, and **G** upstream are strong "hole-and-wave" features, and the name "Crystal Hole" is no longer uniquely definitive. At discharges below 5,000 cfs, a rock can be seen at the position of the Old Crystal Hole. In the diverging section of the rapid, a large eddy can produce a beach at **K**, if sediment is available in the water. The flow is relatively slow in the diverging section of the rapid until the channel splits around the rock garden (**L**, fig. 5).

Streamlines (the paths of floats launched through the rapid) and water-surface velocities were determined from Super-8 motion pictures taken from the camera station shown (figs. 6, 7); because of logistical difficulties and the hazards in this rapid, the streamlines in this map cover less of the rapid than do streamlines on other maps in this series. The floats and experimental technique are described in Kieffer (1987). The floats were launched upstream of the rapid, about at the place where the streamlines begin on the map. Each velocity numeral shown along a streamline (in units of meters/second, m/s) refers to the section of streamline between large dots. The different dash-dot patterns distinguish the different streamlines.

Two sets of floats were launched: one set, whose trajectories are shown in figure 6, was launched when the discharge was approximately 7,000 cfs, very close to the discharge of 5,000 cfs portrayed on the base map of figure 6. Another set was launched when the discharge was 17,000 cfs; a base map is not available for this discharge, but the wave structure in the central part of the rapid is generally similar to that at 30,000 cfs, so these streamlines are shown on the base map for 30,000 cfs in figure 7. In comparing the two figures, the reader should note that velocities are higher and the lateral range of streamlines is broader at 17,000 cfs than at 5,000 cfs. The highest velocities occur near the top of the most tightly constricted part of the rapid where the drop in water-surface elevation is the steepest. Although Crystal Rapids is the most tightly constricted and steepest rapid on the river, the velocities measured are not as high as have been measured in some other rapids. The strong waves and turbulence associated with the constriction, and with drag against rocks and their associated waves, actually seem to produce slower velocities than in rapids where there are fewer waves (compare with Hermit).

The discharges in all cross sections (fig. 4) are referenced to the shoreline at 5,000 cfs (but are based on the velocity data obtained for 7,000 cfs; experimental uncertainty precludes more detail in the calculations). Depths were not measured directly but were obtained from continuity relations by methods described in Kieffer (1987), except for cross section *T–T′* for which fathometer data obtained approximately 150 m upstream at a similar cross section were used. For cross sections *U–U′*, *V–V′*, *W–W′*, and *X–X′*, velocities were measured, so depth could be calculated from the continuity relations (Q=ūwD, where Q is discharge, ū is velocity, w is channel width, and D is average depth; see Kieffer (1987) for details). For cross sections *Y–Y′* and *Z–Z′*, velocity data were not obtained; thus, in order to estimate hydraulic conditions, depths were estimated to be 1 m because boulders of this diameter are typically showing or nearly showing at 5,000 cfs. With this assumption for these two cross sections and for cross section *T–T′*, velocity could then be obtained from the continuity relation. In the discussion below concerning Froude numbers, the relatively large uncertainties introduced in estimating conditions in *Y–Y′* and *Z–Z′* needs to be kept in mind.

From the assumptions and data described above, a Froude number can be calculated for flow in the cross sections shown. The Froude number, $Fr=\bar{u}/(gD)^{1/2}$ (g is the acceleration of gravity), is a dimensionless measure of the relative importances of inertial versus potential energy. The Froude number was calculated for each cross section from the measured and inferred depths and velocities. Froude numbers less than 1 indicate subcritical flow dominated by potential energy, and Froude numbers greater than 1 indicate supercritical flow dominated by kinetic energy. Standing waves are stable features in the flow if the Froude number exceeds 1.

The area shown on these maps begins (left side of the map) in the backwater above Crystal Rapids. In this backwater (for example, at cross section *T–T′*), the low velocity and relatively great depth give a Froude number of only 0.006, typical of backwaters along the river at low discharges. The river accelerates rapidly between this cross section and *U–U′*, reaching a velocity of 5 m/s and a Froude number of 1.7 on the tongue in this convergent part of the rapid. These high average flow velocities are maintained through *V–V′*. Immediately downstream of *V–V′* are several waves (**E**, **F**, and **G** in fig. 5) that affect the flow; although these waves are not as strong at 7,000 cfs as they are at higher discharges, they are sufficiently strong to slow down the floats between *V–V′* and *W–W′*. The Froude number between *W–W′* and *X–X′* is approximately unity, increasing toward wave **J** just upstream from *X–X′*. Below this wave the Froude number decreases to 0.6 at *Y–Y′* (remember the above discussion about the uncertainty of the data for *Y–Y′* and *Z–Z′*). Below *Y–Y′*, the river splits around the "rock garden" (as shown on fig. 1 and in *Z–Z′*, fig. 4), and the Froude number appears to be slightly greater than unity in the two channels north and south of the rock garden.

The fathometer traverse done in the backwater above the rapid at *T–T′* shows that the river bottom has an average elevation of 703 m. The bottom rises across the debris fan to about 705-m elevation at *U–U′* and drops back to about 703.5m elevation at *V–V′*, to about 700-m elevation at *W–W′*, *X–X′*, and *Y–Y′*. The two channels in *Z–Z′* have an estimated elevation as low as 697 or 698 m. This decrease in bed elevation between the backwater and the downstream rock garden is unusual compared with other rapids studied (see, for example, the map of House Rock Rapids I–1897–A; Hance Rapids, I–1897–C; and Horn Creek Rapids, I–1897–E).

In spite of relatively large uncertainties arising from the uncertain nature of the channel geometry and roughness, the calculated Froude numbers indicate that the flow changes from subcritical conditions (Fr<1) upstream of the constriction to supercritical conditions (Fr>1) in the convergence at the top of the rapid and constriction. The flow changes back to critical conditions (Fr=1) below the steep top section, then to supercritical conditions as the second wave is approached (just upstream of *Y–Y′*) and back to subcritical (Fr<1) conditions in the diverging section of the rapid. The flow then goes back to supercritical conditions as the channel narrows and splits to go around to rock garden in the lower part of the rapid, and only downstream of the rock garden (to the right of the mapped region) does the flow return to ambient subcritical conditions that characterize the main channel outside of rapid.

In general, the correlations between low and high Froude numbers and regions of the river with and without large standing waves are quite good. For example, the high Froude numbers calculated between *U–U′* and *W–W′* are in the region of the large standing waves **E**, **F**, and **G** (fig. 5) at the top of the rapid; even higher Froude numbers probably would have been calculated if the floats had not been slowed by hitting the waves in this region. Similarly, the acceleration toward high Froude numbers just in front of wave **J** at *X–X′* is consistent with the existence of supercritical flow in front of a wave (interpreted as a hydraulic jump), which then slows the flow back to low Froude numbers.

The flow pattern at Crystal Rapids since 1983 has been determined primarily by the severe constriction and steep drop in elevation at the head of the rapid; this flow pattern is dramatically different than that before 1983. (For a general discussion of the flow patterns in rapids, see Kieffer, 1985; 1987). Crystal Rapids is unique compared with other rapids on the Colorado River in that it has had both a major tributary flood, in December 1966 after Glen Canyon Dam closed, and a major main-stem flood (92,000 cfs in 1983) since blockage of the river by the debris flow. The two photographs in figure 8 show how severely the 1966 flood constricted the river at Crystal Rapids. Measurements obtained on photographs taken in 1977 showed that, at its narrowest point, the river in Crystal Rapids was only 0.25 of the width upstream in the backwater (in contrast to most rapids where the constriction is about one-half). This severe constriction was the cause of unusual conditions that developed in Crystal Rapids in 1983 (Kieffer, 1985).

Because of the severity of the constriction, strong hydraulic jumps (transitions between supercritical and subcritical flow) could develop in Crystal under certain discharge conditions. In 1983, when, because of the high level of water in Lake Powell and rapid snowmelt, the discharge through Glen Canyon Dam had to be raised above the normal power plant discharges (maximum of about 30,000 cfs), a strong hydraulic jump developed in Crystal. When the discharge was between 50,000 and 70,000 cfs, this wave was between 15 ft (4.5 m) and 20 ft (6 m) high, and it spanned most of the navigable width of the river. As the discharge increased toward 92,000 cfs, the height of the wave decreased because flow velocities became so high that lateral and headward erosion of the river channel could occur (see Kieffer, 1985, for a much more detailed discussion of this problem).

The current configuration of the rapid shown in figures 1–3 reflects the erosion that occurred in 1983: the river is wider on the north shore in the vicinity of cross section X–X′ (and a rather steep-cut face can be seen on the debris fan in this area, as reflected in the steep contours shown upstream of the two boats at beach **K**), and the fall through the rapid is much more severe at the top because the headward erosion appears to have proceeded upstream well above Slate Creek. Therefore, the drop through the rapid that used to be spread out between the tongue (**D**) and the Old Crystal Hole (**J**) is now largely concentrated above Slate Creek. It is interesting to speculate that if the 1983 discharges of 92,000 cfs had been maintained longer, or if they had been slightly higher, the process of headward erosion may have breached the Crystal Creek debris fan, allowing partial drainage of the backwater. In such a case, Boucher Rapids may have once again become a more substantial rapid. This speculation illustrates the influence of rapids on backwaters and on other rapids.

The geometry of the river channel at Crystal Rapids, its relation to the debris fan from Crystal Creek, and the changes in these relations between 1966 and 1983 have given us some clues about how the Colorado River and its debris fans maintain geomorphic equilibrium. These relations are summarized in figure 9. Episodic floods throughout geologic time emplace debris fans into the river channel; a time when an old debris fan (fig. 9*A*) is just about to be covered by a fresh debris flow has been selected as a reference starting time. A debris flow (fig. 9*B*) may be large enough to temporarily pond water behind the debris "dam", forming a "lake". As water spills over this dam, a steep "waterfall" may be formed. This is probably an ephemeral condition, lasting only a few hours or days, because the Colorado River would quickly cut a channel through the distal end of the loosely consolidated material of such a debris fan (fig. 9*C*). Floods of different sizes enlarge the channel (figs. 9*C*–*E*), and rocks from the debris fan are episodically carried downstream to form the rock gardens below the rapids. This process produces the typical backwater-rapid-rock garden configuration seen at most rapids along the river. Cross sections along the thalweg (fig. 9*F*) through the debris fan show the fan's evolution through the sequence represented in figures 9*A*–*E*. This sequence (figs. 9*B*–*E*) is repeated over and over, typically with a time scale of decades to centuries between tributary floods. Since the geomorphic equilibrium configuration of the Colorado River channel depends on the number and size of small, medium, and large floods in the main channel, the geomorphic relations will be different under the controlled discharge conditions of Glen Canyon dam than under the natural discharges that existed before the dam was closed.

To summarize, the most significant hydraulic features in Crystal Rapids are waves caused by the severe constriction of the channel and by some individual rocks. The hydraulic features of Crystal Rapids reflect a dynamic equilibrium between the flow in the Colorado River channel and flooding events in Crystal Creek (and possibly Slate Creek). The configuration of the channel bottom depends not only on the bedrock topography and the contribution from the rockfalls and tributary floods, but also on the transient sediment load of the river. The channel configuration changes with time, both gradually and catastrophically.

REFERENCES

Cooley, M.E., Aldridge, B.N., and Euler, R.C., 1977, Effects of the catastrophic flood of December 1966, North Rim Area, Eastern Grand Canyon, Arizona: U.S. Geological Survey Professional Paper 980, 43 p.

Kieffer, Susan Werner, 1985, The 1983 hydraulic jump in Crystal Rapid: Implications for river-running and geomorphic evolution in the Grand Canyon: Journal of Geology, v. 93, p. 385–406.

Kieffer, Susan Werner, 1987, The rapids and waves of the Colorado River, Grand Canyon, Arizona, U.S. Geological Survey Open-File Report 87–096.

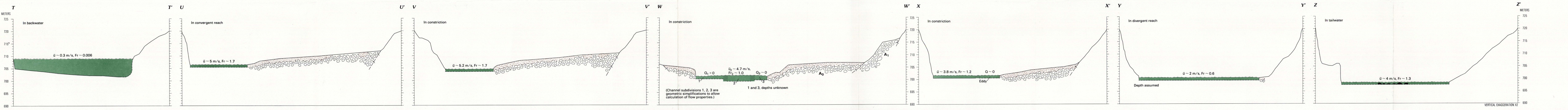

EXPLANATION

Channel boundary—Dashed where estimated

—?—?— Approximate contact

Q Discharge

Fr Froude number

ū Average flow velocity, in meters per second

Debris fan

Sand

Water

Rock

Shear zone in the flow

Figure 4—CROSS SECTIONS SHOWN ON FIGURE 5

SCALE 1:1 000

100 0 100 200 300 FEET

10 0 10 20 30 40 50 60 70 80 90 METERS

CONTOUR INTERVAL 1 METER

INTERIOR—GEOLOGICAL SURVEY, RESTON, VA—1988

Hydraulic data collected in October–November 1985 by Susan Werner Kieffer, assisted by Margie Marley

Contour lines compiled on analytical stereoplotters at the U.S. Geological Survey, Flagstaff, Arizona, from aerial photographs flown in 1984 by the Bureau of Reclamation, Series GCES

Airbrush portrayal of hydraulic features by Patricia Hagerty Gray, U.S. Geological Survey

Prepared on behalf of the Bureau of Reclamation under Interagency Acquisition No. 6–AA–40–04190

U.S. GEOLOGICAL SURVEY RESTON, VA.
MAR 6 1990
LIBRARY